Does the TauD Enzyme Always Hydroxylate Alkanes, While an Analogous Synthetic Non-Heme Reagent Always Desaturates Them?

ARTICLE *in* JOURNAL OF THE AMERICAN CHEMICAL SOCIETY · DECEMBER 2010

Impact Factor: 12.11 · DOI: 10.1021/ja107339h · Source: PubMed

3 AUTHORS:

Usharani Dandamudi
Central Food Technological Research Instit…
27 PUBLICATIONS **314** CITATIONS
SEE PROFILE

Deepa Janardanan
Central University of Kerala
22 PUBLICATIONS **567** CITATIONS
SEE PROFILE

Sason Shaik
Hebrew University of Jerusalem
528 PUBLICATIONS **20,823** CITATIONS
SEE PROFILE

J|A|C|S COMMUNICATIONS

Published on Web 12/20/2010

Does the TauD Enzyme Always Hydroxylate Alkanes, While an Analogous Synthetic Non-Heme Reagent Always Desaturates Them?

Dandamudi Usharani, Deepa Janardanan, and Sason Shaik*

Institute of Chemistry and the Lise Meitner-Minerva Center for Computational Quantum Chemistry, The Hebrew University of Jerusalem, 91904 Jerusalem, Israel

Received August 15, 2010; E-mail: sason@yfaat.ch.huji.ac.il

Abstract: This theoretical work addresses the mechanistic switch between hydroxylase (alcohol formation) and desaturase (olefin formation) activities during alkane oxidation by two non-heme high-valent oxoiron reagents, the enzyme taurine:α-ketoglutarase dioxygenase (TauD) and the synthetic shape-selective catalyst (TpOBzFe), toward cyclohexadiene, cyclohexane, cyclopentane, and ethane. As we show, the desaturase/hydroxylase steps obey unique orbital selection rules, and the mechanistic switch is determined by intrinsic reactivity factors that depend on the ligand-sphere flexibility of the oxoiron species, the substrate, and the spin states of the reaction pathways. Testable predictions are outlined.

This communication addresses factors that control the mechanistic bifurcation (Scheme 1a) encountered during the reactivity of oxoiron $L_nFe(IV)=O$ species of non-heme enzymes and their synthetic models with alkanes.[1] Thus, while the key reaction of $L_nFe(IV)=O$ is H abstraction from the alkane,[1] the subsequent step poses an interesting mechanistic dilemma: the FeOH/radical species (Scheme 1a) may either undergo rebound[2] to yield an alcohol complex or produce an olefin by a second H abstraction (or successive electron transfer followed by carbocation deprotonation).[1b,c,e,g,h,3−5] As such, *will the resulting FeOH/radical act as a hydroxylase, a desaturase, or both*? Also, what is then the root cause of the switch between the two pathways? These are questions of intense current interest.[1c,3,6,7] As we show herein, the desaturase/hydroxylase steps follow orbital selection rules that are the opposite of those for the first H-abstraction step,[8a−c] and the mechanistic partition in Scheme 1a is determined by definitive intrinsic reactivity factors that depend on the nature of the oxoiron species, the substrate, and the spin states of the reaction pathways.

While this mechanistic dichotomy appears in all iron enzymes[1b,f,g,3,4] and synthetic models,[1c,e,h] its underlying reasons are complex and may depend on intrinsic features of the active oxoiron complex and of the substrate,[1c,d,f,h,4−6] on the metal (Mn vs Fe),[7] and on extrinsic factors such as the substrate/radical binding in the protein pocket.[3,7] Additionally, most of the non-heme Fe(IV)=O reagents involve two closely lying spin states that have different behaviors.[8,9] It is therefore clear that this multidimensional problem must be resolved step by step. For this reason, we focus herein on two related systems in which this dichotomy is manifested, which are depicted as **1** and **2** in Scheme 1b. **1** is the active species[1b] of the taurine:α-ketoglutarase dioxygenase (TauD) enzyme, while **2** is derived from the shape-selective catalyst, abbreviated as TpOBzFe ([Fe(Tp^{Ph2})OBz], where Tp^{Ph2} = hydrotris(3,5-diphenylpyrazol-1-yl)borate and OBz = benzoate), which oxidizes substrates upon O_2 feeding, as in TauD.[1h,10] It should be noted that **1** and **2** have carboxylate arms that can be either bidentate or monodentate,[8b,d]

Scheme 1. (a) To Be Hydroxylated or Desaturated or Both? (b) Investigated Oxoiron Species (**1** and **2**); (c) Investigated Substrates (**S1**−**S4**); the Derived Radicals are Referred to as **S1**·−**S4**·

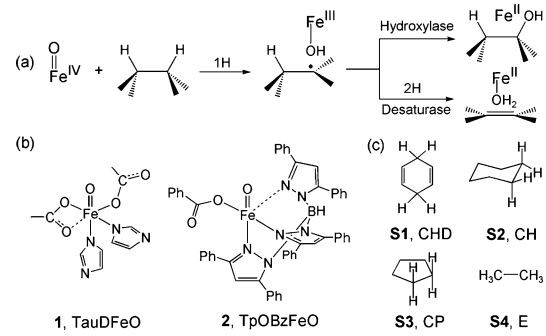

and furthermore, both show a preference for the quintet ($S = 2$) state reactivity over the triplet ($S = 1$) state.[8b,d,f] Nevertheless, **1** hydroxylates the α-C−H of taurine,[1b] but it has never been reported to perform desaturations. On the other hand, **2** has been reported to generally desaturate alkanes.[1h] Are these roles exclusive, or are they substrate- and oxidant-dependent?

It is entirely possible that TauD acts as a hydroxylase toward taurine because the protein exerts a tight control on the movement of the substrate and the radical, which can thereby only rebound.[3b,7] But this reasoning would not apply to **2**, and hence, there could also be intrinsic factors that control the hydroxylase/desaturase activities of both **1** and **2**. To explore these intrinsic factors, we investigated the reactivities of **1** and **2** toward the substrates **S1**−**S4** (Scheme 1c) using density functional theory (DFT) calculations at the UB3LYP level. **S1** and **S2** are frequently used in mechanistic studies,[1c,g,h,5] and **S3** is known to be activated by **2**,[1h] while **S4** has been used as a mimic of taurine.[8d−f]

As in analogous studies,[8b,d] geometries were optimized herein with the LACVP basis set (B1). Pathways were ascertained by intrinsic reaction coordinate (IRC) calculations[11] using Gaussian 09.[12a] Energies were corrected with LACV3P+* (B2) and solvation [$\varepsilon = 5.71$ (**1**) and 2.28 (**2**)] using the Poisson−Boltzmann solver method in Jaguar 7.6.[12b] Since B3LYP lacks dispersion interactions,[13] we added the corresponding energy correction (D2 in Gaussian).[12a] Since the first H abstractions in **1** and **2** were studied previously,[8b,d] we shall not describe the corresponding details [however, see the Supporting Information (SI)]; we shall refer to the first H abstraction only when it contrasts with or highlights the unique features of the second H abstraction nascent from the FeOH/radical intermediates. No electron transfer from the substrate radical to FeOH, as reported for P450,[5a] occurred herein. The SI includes all of the data, while below we discuss the key results.

Figure 1 shows generic energy profiles for the $S = 2$ and $S = 1$ states. The $S = 1$ surface lies typically 1−18 kcal/mol above the S

10.1021/ja107339h

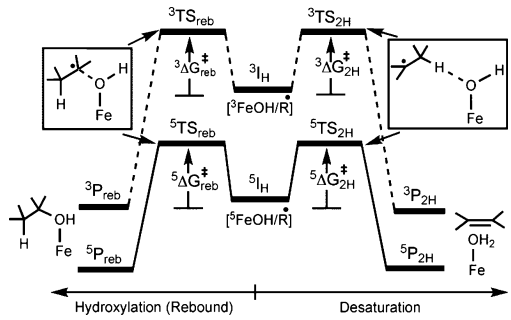

Figure 1. Generic energy profiles for hydroxylation vs desaturation, starting from the $^{2S+1}\mathbf{I}_H$ intermediates formed by initial H abstraction.

= 2 surface on the free-energy scale. Comparison of the $S = 1$ and $S = 2$ results are important because many synthetic oxoiron complexes have $S = 1$ ground states[1c−e,8a−g] and because the two spin states will be shown to obey unique orbital selection rules and barrier-controlling factors.

Table 1 collects the free-energy barriers for the reactions of different substrate radicals with **1-OH** and **2-OH**. The table reveals the dependence of the barriers on the identity of the substrate, the Fe−OH species, and the spin state. Thus, the barriers for the second H abstraction by the present Fe−OH species are not negligible, as recently found for Mn−OH oxidants[7] and as occasionally deduced from common kinetic isotope effects for the two products.[3,4] In fact, the barriers in Table 1 are lower than the barriers for the first H abstraction (e.g., by only 3−4 kcal/mol on the $S = 2$ surface; see Figures S1−S7 in the SI).

Furthermore, as expected,[1c−g,6,14,15] the barriers for the second H abstraction within each spin state follow roughly (but not regularly) the C−H bond strengths, being the smallest for **S1·** and larger for **S2·**−**S4·**. The rebound barriers are also substantial and are invariably the largest for **S1·**, wherein the cyclohexadienyl radical is delocalized and loses its delocalization energy upon rebound. The trends in the barriers are similar for the two spin states, but the barriers for the processes on $S = 1$ are larger. Finally, consideration of the entire data set shows that free-energy relationships are not obeyed, because other factors obviously play a role in the reactivity.[15]

Let us inspect now the substrate-dependent desaturation versus rebound selectivity for the $S = 2$ state. The dispersion correction generally lowers the rebound barriers but does not reverse the relative rebound/second H abstraction (reb/2H) barriers. Thus, the results in Table 1 predict that **S1·** should undergo exclusive desaturation with both reagents. This result is in accord with experimental evidence for **2-OH**,[1h] while for **1-OH** the desaturation is reminiscent of the demonstration by Lipscomb et al.[1g] of desaturase activity toward **S1·** for methane monooxygenase, which is a native hydroxylase. With ethyl radical (**S4·**), both **1-OH** and **2-OH** are predicted to yield dominant hydroxylase activity. This hydroxylase activity for **1** (TauD) is in accord with the activity experimentally observed with the native substrate taurine.[1b] At the same time, the calculations predict a novel hydroxylase activity for TpOBzFe (**2**) toward **S4·**, which could also be applicable to other straight-chain alkanes. With cyclohexyl radical (**S2·**), **1-OH** exhibits mixed reactivity with a slight preference for rebound on the DFT free-energy scale, which further increases upon dispersion correction. Similarly, for **1-OH** + **S3·**, the calculations without and with dispersion predict predominant hydroxylase activity. The shape-selective reagent **2** does not oxidize **S2**,[1h] and therefore, we did not study this reaction. However, **2** is known to react with cyclopentane (**S3**). While the corresponding products were not identified,[1h] on the basis of the exclusive desaturation of cyclohexene and 9,10-dihydroanthracene it was assumed by the authors[1h] that this is true also for other substrates, including **S3**.[1h] Table 1 predicts mixed reactivity, with some preference for desaturation, but as discussed next, this is induced by the flexibility of the coordination sphere of **2-OH**.

The above trends highlight the different intrinsic reactivities of **1** and **2** in the $S = 2$ state. Thus, the coordination shell of TauD−OH (**1-OH**) is somewhat more rigid than that of TpOBzFe−OH (**2-OH**), and by-and-large **1-OH** can maintain six coordination around the iron. On the other hand, **2-OH** has a more flexible coordination sphere, causing the reaction mode of **2-OH** with **S3·** to be controlled by the flexibility of the benzoate ligand. Indeed, as shown in Figure 2, the initial $^5\mathbf{I}_H$ intermediate, which (by the IRC criterion) could have potentially mediated a hydroxylase activity at a low barrier [2.7 (1.9) kcal/mol], collapses preferentially to the more stable $^5\mathbf{I}_{2H}$ intermediate that by the IRC test mediates desaturation of **S3·**.

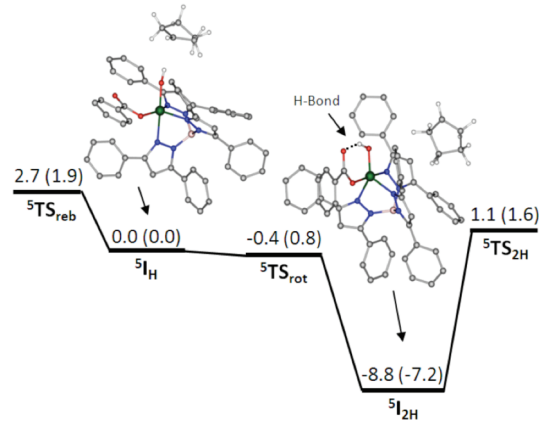

Figure 2. **2-OH/S3·** intermediates and the potential energy profile connecting them, leading to desaturation and hydroxylation. Relative energies (kcal/mol) at the B2 + solv + G_{corr} (B2 + solv + G_{corr} + D) level are given.

It is seen that $^5\mathbf{I}_{2H}$ is formed by benzoate rotation, which forms thereby a favorable H-bonding interaction with the FeOH moiety. As such, $^5\mathbf{I}_{2H}$ is the common intermediate for the two processes, with $\Delta G_{reb}^{\ddagger}/\Delta G_{2H}^{\ddagger}$ barriers of 11.5/9.9 (9.1/8.8 with D correction) kcal/mol, and we conclude that **2-OH** should exhibit mixed hydroxylase/desaturase activity toward **S3·**. It should also be noted that $^5\mathbf{I}_{2H}$ and $^5\mathbf{I}_H$ differ here in their orientation, as found previously for the reactions of Mn−OH complexes.[7]

The reactivities of **1-OH** and **2-OH** toward **S1·**−**S4·** thus exhibit a clear expression of intrinsic factors, such as C−H bond strength, radical delocalization, ligand-sphere flexibility, and possibly also steric effects. Importantly, however, there is also selectivity that derives from the electronic reorganization during the two processes nascent from $^{5,3}\mathbf{I}_H$. Thus, as shown in the electron-shift diagrams[8a,b] (exemplified in Scheme 2a,b for six-coordinate $^{5,3}\mathbf{I}_H$ species), the reb/2H competition is accompanied by competing electron shifts, from either the ϕ_C orbital on the radical center or the σ_{CH} orbital of the adjacent C−H bond to the iron d orbitals. These shifts occur to the lower-lying $\pi^*_{xz/yz}$ orbital for $S = 2$ (Scheme 2a) and to the higher-lying $\sigma^*_{z^2}$ orbital for $S = 1$ (Scheme 2b). Because of the high energy required for promotion to $\sigma^*_{z^2}$ vis-à-vis only a small gain in exchange stabilization,[8b] the barriers are generally higher for $S = 1$ than for $S = 2$, as shown in Table 1.

Additionally, the 2H/reb competition depends on the $\sigma_{CH}-\phi_C$ energy gap, $\Delta E(\sigma_{CH}-\phi_C)$, and the proximity of these two orbitals

Table 1. Free-Energy Barriers and Reaction Free Energies (kcal/mol)[a] for Rebound and Desaturation Processes Nascent from the $^{2S+1}\mathbf{I}_H$ Intermediates (FeOH/R$^\bullet$) for **1-OH** and **2-OH**

	$S = 2$		$S = 1$	
model	$\Delta G^{\ddagger}_{reb}/\Delta G^{\ddagger}_{2H}$	$\Delta G_{reb}/\Delta G_{2H}$	$\Delta G^{\ddagger}_{reb}/\Delta G^{\ddagger}_{2H}$	$\Delta G_{reb}/\Delta G_{2H}$
1-OH + **S1**$^\bullet$	10.1/0.0 (7.5/0.0)	−17.8/−53.2	16.8/8.9 (17.0/9.9)	−14.7/−49.5
1-OH + **S2**$^\bullet$	5.5/6.8 (5.0/8.2)	−41.7/−39.2	7.6/12.6 (7.3/13.3)	−40.8/−39.3
1-OH + **S3**$^\bullet$	4.1/8.3 (2.6/9.1)	−40.1/−37.4	9.7/15.9 (6.3/15.2)	−36.3/−36.0
1-OH + **S4**$^\bullet$	4.6/7.6 (3.2/6.4)	−46.2/−35.8	6.9/16.4 (6.9/18.6)	−43.0/−35.8
2-OH + **S1**$^\bullet$	10.1/0.0 (8.4/0.0)	−19.5/−53.7	20.0/10.5 (18.1/9.4)	−3.9/−36.5
2-OH + **S3**$^\bullet$	11.5/9.9[b] (9.1/8.8[b])	−46.1/−31.3	17.3/18.3 (14.2/15.5)	−39.6/−31.1
2-OH + **S4**$^\bullet$	4.4/7.4 (2.9/6.2)	−44.4/−39.9	10.5/14.2 (12.2/14.1)	−37.4/−36.7

[a] Barriers and reaction energies relative to the corresponding $^{2S+1}\mathbf{I}_H$. In parentheses are barriers with dispersion corrections (B2 + solv + G_{corr} + D). [b] Barriers from $^5\mathbf{I}_{2H}$ (see Figure 2).

Scheme 2. Electron-Shift Diagrams for Six-Coordinate **1-OH** and **2-OH** during Desaturation and Rebound in (a) $S = 2$ and (b) $S = 1$ and for **1** and **2** during the First H Abstraction in (c) $S = 2$ and (d) $S = 1$

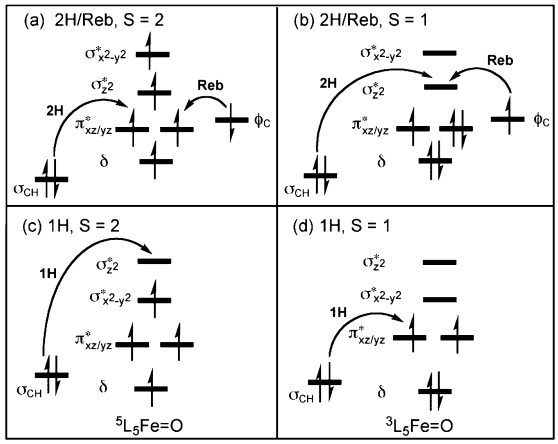

to the accepting orbital $\pi^*_{xz/yz}$ (Scheme 2a). For a series of substrates and a given oxidant, this competition depends on $\Delta E(\sigma_{CH}-\phi_C)$ as well as on the extent of radical delocalization. Our calculated $\Delta E(\sigma_{CH}-\phi_C)$ values [102.1, 100.5 91.1, and 133.7 kcal/mol for **S1**$^\bullet$−**S4**$^\bullet$, respectively] show that the gap is largest for **S4**$^\bullet$ and significantly smaller for **S1**$^\bullet$−**S3**$^\bullet$. Thus, for a radical like ethyl (**S4**$^\bullet$) in which σ_{CH} is lower in energy than ϕ_C, the two reagents should exhibit a preferential hydroxylase activity for both oxidants. However, for **S1**$^\bullet$ with a smaller orbital gap and higher σ_{CH}, the desaturase activity should be more pronounced and further augmented by the aromatic stabilization of the benzene product. Simultaneously, the delocalized ϕ_C for **S1**$^\bullet$ raises the rebound barriers. Therefore, desaturation should predominate for the reactions of both **1** and **2** with **S1**. The substrates **S2** and **S3** represent intermediate situations, and thus should tend more toward mixed hydroxylase/desaturase activities. The differences reported herein for **1** and **2** result primarily from the ligand-sphere flexibility of the latter and the ability of its cleft to interact with the substrate radical rather than from any apparent electronic factors.

The electron-shift diagrams in Scheme 2 also allow the orbital selection rules that predict the transition-state structures to be derived *on the basis of the overlap of the electron-donating and -accepting orbitals*.[8a,b] Since it is commonly accepted that the first H abstraction proceeds via the σ trajectory with an upright structure,[8a,b,d−h,16,17] it is important to demonstrate that the orbital selection rules for the second H abstraction are *precisely opposite to those derived previously*[8a,b] *for the first H abstraction process and also unique and spin-state-specific*. Therefore, Scheme 2 includes both H-abstraction and rebound processes in the two spin states.

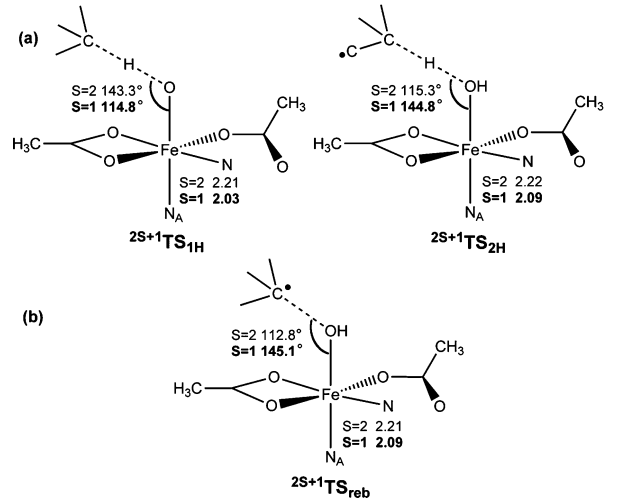

Figure 3. Key geometric features of (a) $^{2S+1}\mathbf{TS}_{1H}$ for **1** + **S4** and $^{2S+1}\mathbf{TS}_{2H}$ for **1-OH** + **S4**$^\bullet$ and (b) $^{2S+1}\mathbf{TS}_{reb}$ for **1-OH** + **S4**$^\bullet$.

Thus, on the basis of the donor and acceptor orbitals in Scheme 2, we may predict that for the $S = 2$ state in Scheme 2a, the six-coordinate $^5\mathbf{TS}_{2H}$ will assume a structure that optimizes the overlap of σ_{CH} with the acceptor orbital $\pi^*_{xz/yz}$ and will therefore have a structure with an Fe-O−H angle of ∼120°.[8b] On the other hand, as shown in Scheme 2c, during the first H abstraction in the $S = 2$ process, the electron shifts from σ_{CH} to the $\sigma^*_{z^2}$ orbital, so the corresponding $^5\mathbf{TS}_{1H}$ structure must optimize the overlap of these two orbitals and will therefore assume a conformation with a larger Fe-O−H angle. In contrast, the corresponding triplet structures $^3\mathbf{TS}_{1H}$ and $^3\mathbf{TS}_{2H}$ are predicted to exhibit opposite trends. Thus, according to Scheme 2b, $^3\mathbf{TS}_{2H}$ will assume an upright structure that optimizes the $\sigma^*_{z^2}$ overlap, while $^3\mathbf{TS}_{1H}$ must optimize the $\sigma_{CH}-\pi^*_{xz/yz}$ overlap and will therefore assume a structure with a smaller Fe-O−H angle. Figure 3a exemplifies these transition states for **1** + **S4** (and **1-OH** + **S4**$^\bullet$, and it is apparent that they follow the selection rules of the electron-shift diagrams[8a,b,16] and are state-specific and unique for the $^5\mathbf{TS}_{2H}$ structures.

In a similar fashion, Scheme 2a,b predicts that $^5\mathbf{TS}_{reb}$ and $^3\mathbf{TS}_{reb}$ should exhibit different selection rules and hence also different Fe-O−C angles[8a,g,16] (smaller in $^5\mathbf{TS}_{reb}$ and larger in $^3\mathbf{TS}_{reb}$). The corresponding rebound structures for **1-OH** + **S4**$^\bullet$ shown in Figure 3b are seen to follow these rules. Thus, it is once again apparent that the selection rules are state-specific and unique for the $^5\mathbf{TS}_{2H}$ and $^5\mathbf{TS}_{reb}$ structures of interest.

Of course, the identity of the selection rules depends on the ligand-sphere flexibility of the particular oxidant. As we have already noted, **2-OH** has a flexible benzoate arm (e.g., see Figure 2) and therefore has a greater propensity toward five coordination in comparison with **1**−OH. This propensity is manifested in the *S*

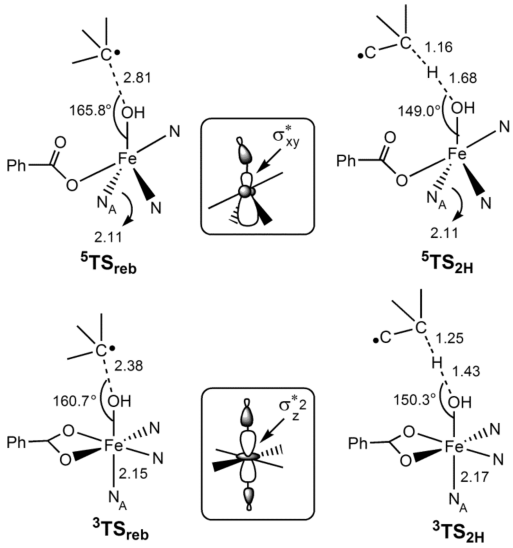

Figure 4. Key geometric features of $^{5/3}$**TS**$_{reb}$ and $^{5/3}$**TS**$_{2H}$ for **2-OH** + **S4·**. The accepting orbitals in the electron-shift diagrams are shown in the boxes.

$= 2$ state, while the $S = 1$ state conserves six coordination. Thus, for **2-OH** with **S1·** and **S4·** for which ^{5}**I**$_H$ assumes a five-coordinate structure with a *basal* Fe−OH bond, the corresponding acceptor orbital is a σ^*_{FeO} type (replacing $\pi^*_{xz/yz}$ as in Scheme 2a). This σ^*_{FeO} orbital lies along the basal Fe−OH direction. At the same time, since the corresponding ^{3}**I**$_H$ species is six-coordinate, the relevant acceptor orbital is still σ^*_z (as in Scheme 2b) and also lies along the Fe−OH axis of the pseudo-octahedral structure. Consequently, for **2-OH** (with **S1·** and **S4·**), the transition states on the two spin surfaces are predicted to exhibit *similar angular orientations because of the different coordination numbers*. Figure 4 exemplifies schematically the corresponding structures for $^{5/3}$**TS**$_{reb}$ and $^{5/3}$**TS**$_{2H}$ for **2-OH** + **S4·**, along with cartoons showing the accepting orbitals. It is seen that while the structures for the two spin states have different coordination numbers, they still obey the orbital selection rules. This is generally the case for other structures found in this study (see Table S2 in the SI). The selection rules seem to be quite compelling and are state- and spin-specific and unique for the $S = 2$ processes.

In conclusion, we can state that although substrate/radical binding in the enzyme could certainly be important,[3,7] in general the switch between hydroxylase and desaturase activity (Scheme 1a) is strongly influenced by intrinsic factors. Some of these factors depend on the substrate, such as its C−H bond strength, its steric bulk, and the delocalization of its radical derived in the first H abstraction. Others depend on the oxoiron reagent, including its spin state and its orbital structure at the $^{2S+1}$**I**$_H$ junction point. In this study, we used oxoiron complexes with similar first coordination spheres and nevertheless observed differences due to the variance in flexibility or rigidity of the coordination spheres of **1-OH** and **2-OH**. The recent results of Hull et al.[7] for the porphyrin Mn−OH reagent show that the barriers for both the 2H and rebound processes are virtually zero and that the switch solely involves barrierless reorientation. Those results,[7] vis-à-vis the present ones, imply that the switch may also be sensitive to the identity of the transition metal. This metal-based effect merits a future stdy.

Interestingly, while the first H abstraction on the $S = 2$ surface follows the upright σ^*_z trajectory,[8a,b,d,f,16−18] the corresponding second H abstraction follows a bent $\pi^*_{xz/yz}$ trajectory, and vice versa for the $S = 1$ state.[8a,b,d,f,16] The same dichotomy applies to the corresponding rebound TSs for the two spin states. These differences between the structural features of the transition states for the two spin states may be expressed in synthetic non-heme oxoiron reagents wherein the ground state of the complex is $S = 1$.[16,17,19] Thus, our study shows that intrinsic factors make a difference!

In addition, the study makes verifiable predictions, such as the desaturase activity of TauD toward cyclohexadiene (**S1**), the hydroxylase activity of TpOBzFe toward ethane (**S4**) or straight-chain alkanes, and the mixed hydroxylase/desaturase activity of TpOBzFe toward cyclopentane (**S3**). Another prediction is that the use of a rigid carboxylate ligand for TpOBzFe (see Figure 2) may lead to significant cyclopentane hydroxylation. These are potential tests of the theoretical results.

Elucidation of both extrinsic and intrinsic factors for TauD will have to be done in the future using the QM/MM methodology.

Acknowledgment. S.S. thanks the ISF (Grant 53/09).

Supporting Information Available: Tables S1−S16, Figures S1−S26, Cartesian coordinates, computational details, and complete ref 12a (as SI ref 4b). This material is available free of charge via the Internet at http://pubs.acs.org.

References

(1) (a) *Acc. Chem. Res.* **2007**, *40* (7), 465−634 (special issue on Dioxygen Activation by Metalloenzymes and Models). (b) Krebs, C.; Fujimori, D. G.; Walsh, C. T.; Bollinger, M. J., Jr. *Acc. Chem. Res.* **2007**, *40*, 484–492. (c) Nam, W. *Acc. Chem. Res.* **2007**, *40*, 522–531. (d) Kim, C.; Dong, Y.; Que, L., Jr. *J. Am. Chem. Soc.* **1997**, *119*, 3635–3636. (e) Xue, G.; de Hont, R.; Münck, E.; Que, L., Jr. *Nat. Chem.* **2010**, *2*, 400–405. (f) Zhou, J.; Kelly, W. L.; Bachmann, B. O.; Gunsior, M.; Townsend, C. A.; Solomon, E. I. *J. Am. Chem. Soc.* **2001**, *123*, 7388–7398. (g) Jin, Y.; Lipscomb, J. D. *J. Biol. Inorg. Chem.* **2001**, *6*, 717–725. (h) Mukherjee, A.; Martinho, M.; Bominaar, E. L.; Münck, E.; Que, L., Jr. *Angew. Chem., Int. Ed.* **2009**, *48*, 1780–1783.
(2) Groves, J. T. *J. Chem. Educ.* **1985**, *62*, 928–931.
(3) For reviews of this bifurcation in non-heme Fe_2O_2-core desaturases, see, for example: (a) Fox, B. G.; Lyle, K. S.; Rogge, C. E. *Acc. Chem. Res.* **2004**, *37*, 421–429. (b) Buist, P. H. *Nat. Prod. Rep.* **2004**, *21*, 249–262. (c) Behrouzian, B.; Buist, P. H. *Curr. Opin. Chem. Biol.* **2002**, *6*, 577–582.
(4) For reviews of this bifurcation in P450, see, for example: (a) Akhtar, M.; Wright, J. N. *Nat. Prod. Rep.* **1991**, *8*, 527–551. (b) Guengerich, F. P. *Chem. Res. Toxicol.* **2001**, *14*, 611–650. (c) Ortiz de Montellano, P. R. *Trends Pharmacol. Sci.* **1989**, *10*, 354–359.
(5) For computational data showing proton-coupled electron transfer in P450, see: (a) Kumar, D.; de Visser, S. P.; Shaik, S. *J. Am. Chem. Soc.* **2004**, *126*, 5072–5073. (b) Hackett, J. C.; Brueggemeier, R. W.; Hadad, C. M. *J. Am. Chem. Soc.* **2005**, *127*, 5224–5237.
(6) Kumar, D.; Tahsini, L.; de Visser, S. P.; Kang, H. Y.; Kim, S. J.; Nam, W. *J. Phys. Chem. A* **2009**, *113*, 11713–11722.
(7) Hull, J. F.; Balcells, D.; Sauer, E. L. O.; Raynaud, C.; Brudvig, G. W.; Crabtree, R. H.; Eisenstein, O. *J. Am. Chem. Soc.* **2010**, *132*, 7605–7616.
(8) For example, see: (a) Shaik, S.; Hirao, H.; Kumar, D. *Acc. Chem. Res.* **2007**, *40*, 532–542. (b) Janardanan, D.; Wang, Y.; Schyman, P.; Que, L., Jr.; Shaik, S. *Angew. Chem., Int. Ed.* **2010**, *49*, 3342–3345. (c) Johansson, A. J.; Blomberg, M. R.; Siegbahn, P. E. M. *J. Phys. Chem. C* **2007**, *111*, 12397–12406. (d) Latifi, R.; Bagherzadeh, M.; de Visser, S. P. *Chem.—Eur. J.* **2009**, *15*, 6651–6662. (e) Godfrey, E.; Porro, C. S.; de Visser, S. P. *J. Phys. Chem. A* **2008**, *112*, 2464–2468. (f) Ye, S.; Neese, F. *Curr. Opin. Chem. Biol.* **2009**, *13*, 89–98. (g) Geng, C.; Ye, S.; Neese, F. *Angew. Chem., Int. Ed.* **2010**, *49*, 5717–5720. (h) Bernasconi, L.; Louwerse, M. J.; Baerends, E. J. *Eur. J. Inorg. Chem.* **2007**, 3023–3033.
(9) For a recent review of two-state reactivity, see: Schwarz, H. *Int. J. Mass. Spectrom.* **2004**, *237*, 75–105.
(10) Ha, E. H.; Ho, R. Y. N.; Kisiel, J. F.; Valentine, J. S. *Inorg. Chem.* **1995**, *34*, 2265–2266.
(11) Gonzalez, C.; Schlegel, H. B. *J. Chem. Phys.* **1989**, *90*, 2154–2161.
(12) (a) Frisch, M. J.; et al. *Gaussian 09*, revision A.02; Gaussian, Inc.: Wallingford, CT, 2009. (b) *Jaguar*, version 7.6; Schrödinger, LLC: New York, 2008.
(13) Grimme, S. *J. Comput. Chem.* **2006**, *27*, 1787–1799.
(14) Mayer, J. M. *Acc. Chem. Res.* **1998**, *31*, 441–450.
(15) Shaik, S.; Lai, W. Z.; Chen, H. *Acc. Chem. Res.* **2010**, *43*, 1154–1165.
(16) Hirao, H.; Kumar, D.; Que, L., Jr.; Shaik, S. *J. Am. Chem. Soc.* **2006**, *128*, 8590–8606.
(17) Decker, A.; Rohde, J.-U.; Klinker, E. J.; Wong, S. D.; Que, L., Jr.; Solomon, E. I. *J. Am. Chem. Soc.* **2007**, *129*, 15983–15996.
(18) Wang, Y.; Han, K. *J. Biol. Inorg. Chem.* **2010**, *15*, 351–359.
(19) Bukowski, M. R.; Kohentop, K. D.; Stubna, A.; Bominaar, E. L.; Halfen, J. A.; Münck, E.; Nam, W.; Que, L., Jr. *Science* **2005**, *310*, 1000–1002.

JA107339H